Structural domains required for channel function of the mouse transient receptor potential protein homologue TRP1β

Michael Engelke[a,1], Olaf Friedrich[a,c,1], Petra Budde[a,1], Christina Schäfer[a], Ursula Niemann[a], Christof Zitt[b,d], Eberhard Jüngling[b], Oliver Rocks[e], Andreas Lückhoff[b], Jürgen Frey[a,*]

[a] *Universität Bielefeld, Fakultät für Chemie, Biochemie II, Universitätsstrasse 25, D-33615 Bielefeld, Germany*
[b] *Institut für Physiologie, RWTH-Aachen, Pauwelsstrasse 30, D-52074 Aachen, Germany*
[c] *Nordmark Arzneimittel GmbH & Co KG, Pinnaualle 4, D-25436 Uetersen, Germany*
[d] *Byk Gulden GmbH, Byk Gulden Strasse 2, D-78467 Konstanz, Germany*
[e] *Max-Planck-Institut für Molekulare Physiologie, Otto-Hahn-Str. 11, D-44227 Dortmund, Germany*

Received 2 March 2002; revised 7 June 2002; accepted 10 June 2002

First published online 25 June 2002

Edited by Maurice Montal

Abstract Transient receptor potential proteins (TRP) are supposed to participate in the formation of store-operated Ca^{2+} influx channels by co-assembly. However, little is known which domains facilitate the interaction of subunits. Contribution of the N-terminal coiled-coil domain and ankyrin-like repeats and the putative pore region of the mouse TRP1β (mTRP1β) variant to the formation of functional cation channels were analyzed following overexpression in HEK293 (human embryonic kidney) cells. MTRP1β expressing cells exhibited enhanced Ca^{2+} influx and enhanced whole-cell membrane currents compared to mTRP1β deletion mutants. Using a yeast two-hybrid assay only the coiled-coil domain facilitated homodimerization of the N-terminus. These results suggest that the N-terminus of mTRP1β is required for structural organization thus forming functional channels.

Key words: Transient receptor potential protein; Coiled-coil domain; Ankyrin-like repeat; HEK293 cell; Patch clamp; Yeast two-hybrid system

1. Introduction

The mammalian TRP1 protein is a member of the growing family of plasma membrane proteins that share substantial homology to the *Drosophila* transient receptor potential protein (TRP) [1–4]. The *Drosophila* TRP and TRP-like (TRPL) proteins form cation channels that carry a light-activated Ca^{2+} current [5]. In mammals, proteins of the TRP family play an important role for Ca^{2+} channels that provide Ca^{2+} influx after stimulation of membrane receptors linked to the phosphoinositide response [6]. Inhibition of TRP expression by antisense cDNA constructs reduced store-operated Ca^{2+} influx (i.e. Ca^{2+} influx in response to depletion of inositol-1,4,5-trisphosphate (IP_3)-sensitive calcium stores) [7–9]. Overexpression of TRP proteins leads to enhanced receptor-mediated Ca^{2+} influx [7,10–13]. However, the mechanisms of TRP channel formation is not understood. Conflicting results have been reported. In particular, overexpressing TRP1 (the mammalian TRP form most widely expressed across different tissues and cell lines [1,14]) resulted in enhanced store-operated Ca^{2+} influx in CHO cells [3] but the conclusion that TRP1 forms store-operated channels has not been confirmed by others [15]. A plausible explanation for the functional differences observed with TRP1 in different cells may be that TRP1 is not a monomeric channel but co-assembles with other proteins (which may or may not belong to the TRP family). Overexpression of TRP1 thus might favor the formation of homomultimeric channels.

Proposed structural features of all TRP proteins include six transmembrane-spanning helices with a putative pore (pp) region between the fifth and sixth transmembrane segment. The N– as well as the C-terminus are localized intracellularly [16]. This situation is analogous to that in voltage-gated Ca^{2+} channels [17] in which each of four internally homologous domains are built out of six transmembrane segments.

Further analysis of the amino acid sequence of TRP1 suggests that co-assembly with other proteins may be facilitated by the N-terminal cytoplasmic tail. This contains a coiled-coil region that is a candidate for multimerization [18] as well as three ankyrin-like repeats (ANK-repeats) that may be sites of interaction with the cytoskeleton [19]. Ankyrin is an adapter protein that plays a major role in the intracellular sorting and restriction of Ca^{2+} homeostasis proteins [20,21]. The importance of the N-terminus in the related proteins TRP and TRPL in *Drosophila* has been demonstrated by heterologous overexpression of the entire N-terminus of TRP and TRPL which cause an inhibition of the TRP-related current [22]. In a similar approach, Groschner et al. [23] showed that overexpression of the N-terminal fragment of TRPC3 in human umbilical vein endothelial cells suppressed thapsigargin-induced Ca^{2+} entry. In the present study we aimed at an experimental validation of the hypothesis that the N-terminal

*Corresponding author. Fax: (49)-521-1066042.
E-mail address: juergen.frey@uni-bielefeld.de (J. Frey).

[1] M. Engelke, O. Friedrich and P. Budde contributed equally to this paper.

Abbreviations: ANK-repeat, ankyrin-like repeat; $[Ca^{2+}]_i$, intracellular free calcium concentration; CCh, carbachol; cc, coiled-coil; ECS, extracellular solution; EGFP, enhanced green fluorescent protein; fura-2-AM, fura-2-acetoxymethyl ester; HEK293, human embryonic kidney cells; IP_3, inositol-1,4,5-trisphosphate; mAb, monoclonal antibody; M_r, relative molecular mass; mTRP, mouse TRP; TRP, transient receptor potential protein; NMDG, *N*-methyl-D-glucamine; pp, putative pore; TRPC, TRP channel

0014-5793/02/$22.00
PII: S0014-5793(02)02971-X

coiled-coil region as well as ANK-repeats are essential for the capability of mouse TRP1β (mTRP1β), which is the 34 amino acid shorter splice variant of mTRP1α, to form functional Ca^{2+} entry channels.

2. Materials and methods

2.1. cDNA constructs and expression vectors

Total RNA was extracted from mouse brain using the High Pure RNA Tissue Kit (Roche). Two primers, 5′-CGCGGGTACC-CACCCGTTTTCCAGCTCG-3′ (sense) and 5′-TCTACAACATC-TAGAAAATGGTTA-3′ (antisense) were designed and used to amplify the full length mTRP1β cDNA (GenBank accession number U95167) using the TITAN One Tube RT-PCR Kit (Roche). In a second round of PCR a FLAG epitope tag (DYDDDDDK) was attached to the C-terminus. The full length clone of mTRP1β was further cloned by use of the inserted *Kpn*I and *Xba*I restriction sites with an attached FLAG tag into the expression vector pIRES2-enhanced green fluorescent protein (pIRES2-EGFP, Clontech). The following primers were used to generate mutants *mtrp1βΔank* (deleted residues 61–176) 5′-CGCGGGTACCCACCCGTTTTCCAGCTCG-3′(sense)/5′-TAATCTGCAGCACAGTGTGACGTTCTCCTCCTTC-ACCTCTCG-3′ (antisense), the resulting PCR-fragment was cloned into the *Kpn*I and *Dra*III sites of *mtrp1β-FLAG*. *mtrp1βΔcc* (deleted residues 212–266), 5′-TAATGTTAACAATCCTGAACCATACAT-CT-3′ (sense)/5′-TAATGTCGACATAGCATAGTGACAAAAC-3′ (antisense) cloned into the *Hin*cII and *Bst*EII restriction sites of *mtrp1β-FLAG* and *mtrp1βΔpp* (deleted residues 508–628), 5′-TA-ATGGGCCCCAAGAGCTTCCAGCTGATAG-3′ (sense)/5′-TAA-TGGGCCCTCTAGATTAATTTCTTGGAT-3′ (antisense), cloned into the second *Apa*I and *Xho*I sites of *mtrp1β-FLAG*. All mutants were verified by cDNA sequencing.

2.2. Preparation of TRP1 reactive antibodies

For expression of the C-terminal cytoplasmic region (amino acids 646–775) of mtrp1β the cDNA was cloned in frame to six N-terminal histidine residues in the expression vector pET32a(+) (Novagene). The mTRP1β-CT fusion protein was expressed in the *Escherichia coli* strain BL21[DE3] (Novagene). The fusion protein was purified under non-denaturing conditions (Novagene) by immobilized metal affinity chromatography with Ni^{2+}-NTA-agarose beads (Qiagen) and used to immunize rabbits (Eurogentec). The IgG fraction was purified using protein A agarose (Amersham Pharmacia Biotech).

2.3. Yeast two-hybrid assay

To generate fusion constructs with the LexA DNA-binding domain or the B42 transactivation domain, the N- and C-terminal cytoplasmic regions (residues 1–331 and 646–775) and the deletion mutants of *mtrp1β-NT* were subcloned into pLexA and pB42AD, respectively (Clontech; [24]). Yeast transformation was performed as indicated by the supplier (Clontech). Briefly, 100 ng of each plasmid (LexA DNA-binding domain or B42 transactivation domain fusion) was used to successively transform the EGY48[p8op-lacZ] yeast strain that harbors the *lacZ* reporter under control of LexA binding sites. Transformants were plated on media lacking uracil, histidine and tryptophan. Cells surviving under this selection were screened for galactose-dependent $lacZ^{+}$ and $LEU2^{+}$ phenotypes by replica plating on galactose/raffinose media lacking glucose, uracil, histidine and tryptophane in the presence of 5-bromo-4-chloro-3-indolyl-β-D-galactoside (X-Gal) or in absence of leucine. The results were examined after 1, 2 and 3 days.

2.4. Stable cell lines and cell culture conditions

HEK293 (human embryonic kidney) cells (ACC305) were obtained from the DSMZ (Braunschweig), and maintained in Dulbecco's modified Eagle's medium (DMEM) containing 4.5 mg/L glucose, 10% heat-inactivated fetal calf serum in a 37°C/5% CO_2 incubator and passaged by treatment with phosphate-buffered saline (PBS)/0.5 mM EDTA. HEK293 cells were transfected with the cDNA constructs cells by using the SuperFect Transfection Reagent (Qiagen) and selected in the presence of 400 μg/ml G418.

2.5. Immunolocalization of mTRP1β and mutants in HEK293 cells

HEK293 cells stably expressing FLAG-tagged TRP1β wt or mutants were grown on poly-D-lysine coated coverslips. Stained were either plasma membranes plus the FLAG epitope of the respective TRP1β, endoplasmatic reticulum plus FLAG epitope or the FLAG epitope alone. After washing once with PBS for plasma membrane staining cells were incubated with 0.25% (v/v) CM-DiI (Molecular Probes) for 4 min at room temperature and 6 min at 4°C. Cells were washed twice with PBS, fixed with 2.5% paraformaldehyde and then treated with PBS/100 mM glycine for 20 min. After permeabilization with PBS/0.2% (w/v) Triton X-100 and blocking for 20 min with PBS/2% bovine serum albumin (BSA) (w/v) the cells were incubated with the primary mouse anti-FLAG monoclonal antibody (mAb) M2 (Sigma) at 3 μg/ml diluted in the same buffer. After washing three times the samples were incubated with Cy5-conjugated goat anti-mouse polyclonal antibody (Dianova) at a 1:150 dilution in PBS/2% BSA (w/v) for 1 h. After washing the endoplasmatic reticulum was stained with 1.5μM Bodipy TR-X thapsigargin (Molecular Probes) for 3 min. After washing twice cells were mounted on glass slides with Mowiol 4-88 (Hoechst). The slides were examined by confocal laser scanning microscopy (Leica TCS SP2) and images were exported to Adobe Photoshop 6.0.

2.6. Immunoprecipitation and immunoblotting

Cells were lysed in 1 ml lysis buffer (10 mM Tris/HCl pH 7.2, 158 mM NaCl, 5 mM Na_2EDTA, 1% (w/v) Triton X-100, 0.5% (w/v) sodium desoxycholate, 0.1% (w/v) sodium dodecylsulfate (SDS), 0.5% (w/v) NP40, protease inhibitors (Roche)). MTRP1β-FLAG-tagged wt and mutants were immunoprecipitated from cleared lysates with 1 μg of polyclonal goat anti-FLAG antibody (OctA-Probe, Santa Cruz, Biotechnologies). Immunocomplexes were captured with Protein G Sepharose (Amersham Pharmacia Biotech), extensively washed with lysis buffer and bound material was eluted by boiling with two-fold concentrated Laemmli buffer [25]. Proteins were separated by SDS−PAGE and transferred semi-wet in 40 mM glycine, 50 mM Tris, 1 mM SDS, 20% (v/v) methanol with 2.5 mA/cm^2 for 90 min onto a PVDF membrane (Millipore). Filters were blocked over night at 4°C with 10% (w/v) skimmed milk powder in PBS (4.3 mM Na_2HPO_4, 1.4 mM KH_2PO_4, 137 mM NaCl, 2.7 mM KCl), probed with 2 μg/ml rabbit anti-mTRP1-CT in PBS/10% (w/v) skimmed milk powder, washed three times with PBS/0.05% (w/v) Tween-20®, subsequently probed with horseradish peroxidase-labelled goat anti-rabbit antibodies (Dianova) and again washed 10 times with PBS/0.05% (w/v) Tween-20®. Bound antibodies were detected using the ECL-detection system (Amersham Pharmacia Biotech). The antibodies were removed by incubating the filters for 30 min at 60°C in 62.5 mM Tris/HCl pH6.8, 2% (w/v) SDS, 100 mM β-mercaptoethanol and washed for at least 2 h with PBS/0.05% (w/v) Tween-20®. Filters were reprobed with the FLAG-tag specific mAb M2 (Stratagene) (1 μg/ml in PBS/10% (w/v) skimmed milk powder) and detected as described above.

2.7. Measurement of intracellular Ca^{2+} concentration

For digital calcium imaging experiments cells were incubated for 48 h on glass-bottomed dishes coated with 0.01% (w/v) poly-D-lysine. Cells were loaded with DMEM containing 5 μM fura-2-acetoxymethyl ester (fura-2-AM, MobiTec) and 0.05% Pluronic F127 (Molecular Probes) at 37°C for 30 min. Subsequently the solution was diluted two-folds with DMEM and cells were incubated for 10 min at 37°C then washed twice with extracellular solution (ECS) composed of 140 mM NaCl, 5 mM KCl, 1 mM $MgCl_2$, 1.8 mM $CaCl_2$ and 10 mM glucose. Before measurements the samples were washed once with ECS containing 0.5 mM EGTA instead of $CaCl_2$ and kept in ECS−EGTA during the measurement. Cells were stimulated after 30 s with 200 μM carbachol (CCh, Sigma) and the extracellular Ca^{2+}-level was restored to 1.8 mM after 4 min. The changes in intracellular fluorescence intensity of fura-2 in EGFP-positive cells were measured using a T.I.L.L. Photonics imaging system (Planegg) coupled to an inverted Olympus IX70 microscope. Data from individual cells were collected following alternating excitation at 340 and 380 nm at 3 or 4 s intervals and detection of the emission at 510 nm. The ratios and intracellular Ca^{2+} concentrations were calculated using the T.I.L.L.-Vision software 3.3 according to Grynkiewicz et al. [26]. R_{min} and R_{max} were determined externally using fura-2 in ECS buffer. Incomplete desesterification of fura-2-AM was excluded in Mn^{2+} quenching experiments [26].

2.8. Electrophysiology

Currents in HEK293 cells showing the fluorescence of EGFP were measured with the patch-clamp technique in the whole-cell mode [27]. The solution in the pipet contained:

10 mM HEPES pH 7.4, 110 mM caesium aspartate, 20 mM CsCl, 20 mM tetraethylamoniumchloride, 2 mM $MgCl_2$, 10 mM EGTA, 0.3 mM ATP. The standard bath solution contained.

10 mM HEPES pH 7.4, 140 mM NaCl, 5 mM KCl, 1.2 mM $MgCl_2$, 1.2 mM $CaCl_2$, 10 mM glucose. The 'NMDG' (*N*-methyl-D-glucamine) solution in Fig. 4 contained 150 mM NMDG instead of NaCl. The solution labelled 'Ca^{2+} (10 mM)' contained: 10 mM HEPES pH 7.4, 130 mM NaCl, 5 mM KCl, 1.2 mM $MgCl_2$, 10 mM $CaCl_2$, 10 mM glucose. The standard holding potential was −60 mV. All experiments were performed at room temperature (19–23°C). The significance of the results was determined using the Mann–Whitney (rank sum) test.

3. Results

3.1. The coiled-coil domain mediates homodimerization of the N-terminus

To identify TRP1 regions that may be involved in homomultimerization, we analyzed protein–protein interaction using the yeast two-hybrid system. As summarized in Table 1, the N-terminal but not the C-terminal cytoplasmic region of mTRP1β mediated a homophilic interaction in yeast. To determine the region responsible for these associations, deletion constructs of the N-terminus lacking either the ANK-repeats (Δank) or the coiled-coil (Δcc) domains were generated and examined for their interaction with the complete N-terminus (see Table 1). This approach revealed that the coiled-coil domain is necessary and sufficient for homodimerization in the yeast two-hybrid system while the ANK-repeats are not required.

3.2. Expression of mTRP1β wild-type and mTRP1β mutants in HEK293 cells

To provide further evidence for the functional role of the N-terminal domains in mTRP1β channels in living cells, mTRP1β wild-type, mTRP1Δcc and mTRP1Δank were expressed in HEK293 cells. A mutant lacking the pp region (Δpp) was included as a negative control (Fig. 1A). Immunoprecipitation with anti-FLAG antibodies and Western blot analysis using rabbit anti-mTRP1-CT antibodies reactive for amino acids 646–775 of mTRP1β and mutants were performed to identify the correct expression of the protein (Fig. 1B). MTRP1β migrates with an apparent molecular mass of approximately 80 kDa, which is about 10 kDa below the calculated relative molecular mass, mM_r, of 90 kDa. A similar observation has been previously reported for *Xenopus* TRP [28] and TRP1 [25]. The mutants reveal a molecular mass reduction according to the number of amino acids deleted from mTRP1β with the exception of mTRP1βΔpp (Fig. 1B) (mTRP1βΔank, 77 kDa; mTRP1βΔcc, 83.5 kDa; mTRP1βΔpp, 76.5 kDa). Apparently, the membrane-spanning regions contribute to the apparent molecular mass reduction, because deletion of transmembrane segments 5 and 6 increased the apparent M_r of mTRP1βΔpp.

In order to prove that all deletion mutants have the same orientation and localization like wild-type mTRP1β immunofluorescence staining with the FLAG-tag specific antibody M2 in permeabilized cells that co-expressed cytoplasmic EGFP (Fig. 1C–E) was performed. Plasma membranes were stained with the lipophilic dye CM-DiI [29] and the endoplasmatic reticulum was stained with Bodipy TR-X conjugated thapsigargin. Wild-type mTRP1β as well as mutants expressing cells show a clear colocalization with the plasma membrane and only partly colocalize with the endoplasmatic reticulum (Fig. 1D,E). In contrast, there is no colocalization of mTRP1β or mutants with EGFP which is only localized in the cytoplasma and nucleus (Fig. 1C). Thus a distinct plasma membrane-associated staining pattern was observed with all mTRP1β constructs expressed in HEK293 cells.

3.3. Ca^{2+} influx in HEK293 cells expressing either wild-type mTRP1β or mTRP1β mutants

HEK293 cells were chosen as heterologous expression system because these cells express muscarinic receptors. Stimulation with CCh leads to a characteristic $[Ca^{2+}]_i$ (intracellular free calcium concentration) response in fura-2-loaded cells. In vector-transfected EGFP-positive cells (controls), application of 200 μM CCh in the absence of extracellular Ca^{2+} induced a transient increase in $[Ca^{2+}]_i$ that declined to the resting level within 150 s (original traces not shown). Readdition of 1.8 mM extracellular Ca^{2+} induced a sustained $[Ca^{2+}]_i$ rise reflecting Ca^{2+} influx. The average maximum value of $[Ca^{2+}]_i$ out of 14 to 20 cells per experiment observed after Ca^{2+} readdition was 300 ± 50 nM (Fig. 2A, number of independent experiments $n = 8$). In HEK293 cells expressing wild-type mTRP1β, this value was raised to 408 ± 39 nM which is significantly ($P < 0.05$) above that observed in control cells (Fig. 2A,B). In contrast to the results with wild-type mTRP1β, expression

Table 1
Identification of the N-terminal interacting domain in mTRP1β

LexA-BD		B42-AD		Reporter gene-activation
mTRP1NT	1–331	mTRP1NT	1–331	+
mTRP1NT	1–331	mTRP1NTΔank	1–60/177–331	+
mTRP1NT	1–331	mTRP1NTΔcc	1–212/267–331	–
mTRP1NT	1–331	mTRP1CT	646–775	–
mTRP1CT	646–775	mTRP1NT	1–331	–
mTRP1CT	646–775	mTRP1CT	646–775	–
mTRP1NT	1–331	vector		–
mTRP1CT	646–775	vector		–
Vector		mTRP1NT	1–331	–
Vector		mTRP1CT	646–775	–

cDNAs coding for the N- and C-terminal cytoplasmic regions of mTRP1β and the respective deletion mutants were tested for their interaction using the yeast two-hybrid assay. Numbering of the amino acids expressed from the constructs refers to the mTRP1β Genbank accession number U95167. Positive interactions are characterized by growth on LEU2-selective media plates and expression of the lacZ gene (lacZ).

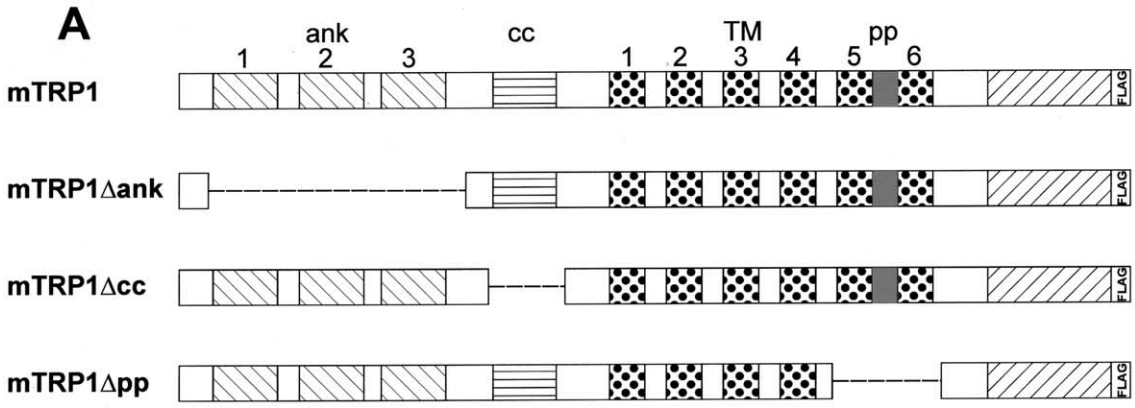
A
ank
cc
TM
pp
1
2
3
1
2
3
4
5
6
mTRP1
mTRP1Δank
mTRP1Δcc
mTRP1Δpp
FLAG

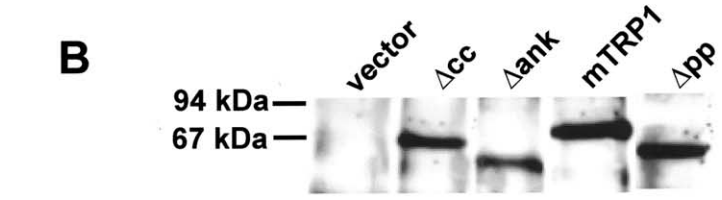
B
vector
Δcc
Δank
mTRP1
Δpp
94 kDa
67 kDa

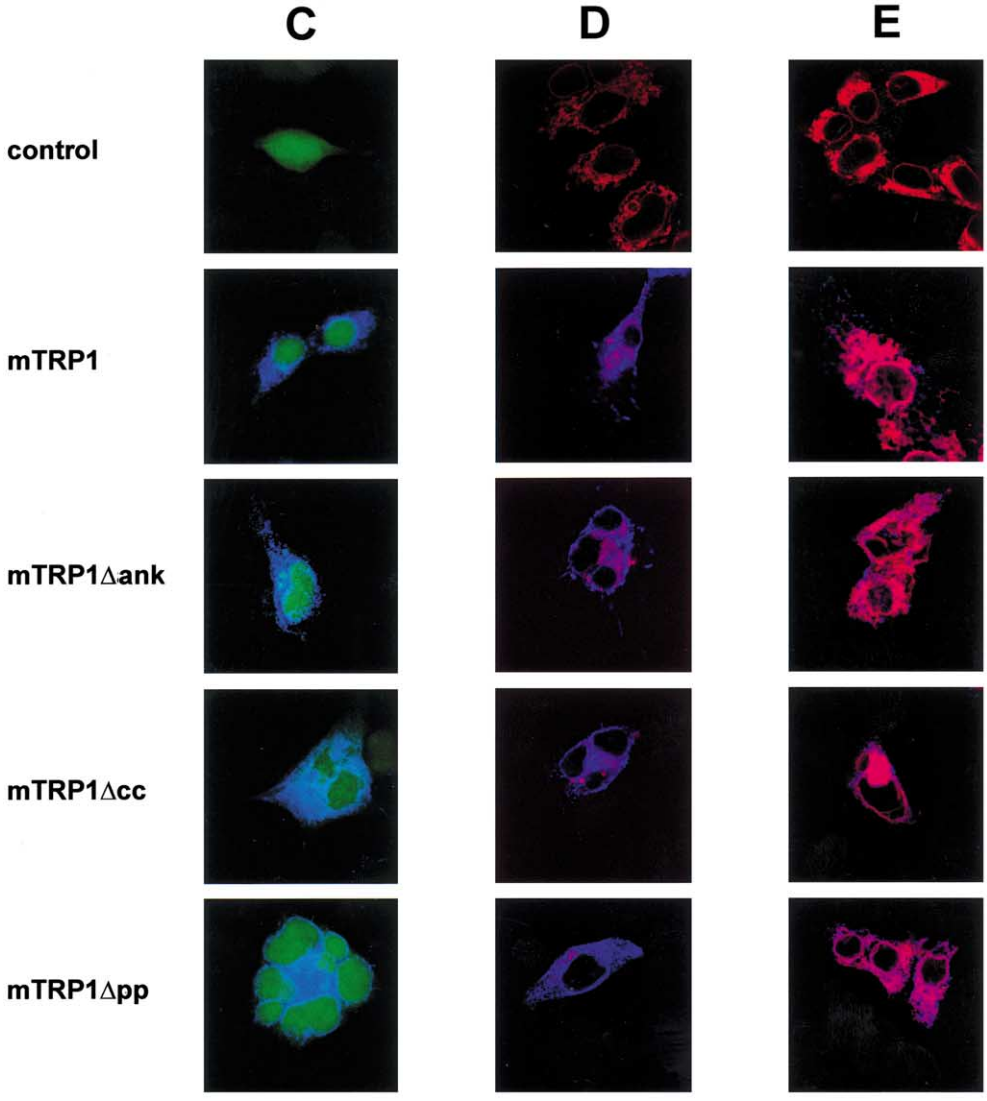
C
D
E
control
mTRP1
mTRP1Δank
mTRP1Δcc
mTRP1Δpp

Fig. 1. Generation, expression and localization of mTRP1β mutants. A: Schematic representation of C-terminal FLAG epitope tagged constructs. Homologous regions are highlighted by identical boxing. ank: ankyrin-repeats, cc: coiled-coil domain, TM: transmembrane segments and pp: putative pore. Deleted regions are indicated by a bar. B: Immunoprecipitation of FLAG-tagged mTRP1β and mutants from stable HEK293 cell clones. Immunoprecipitation was carried out as described in Section 2 using the FLAG-specific antibody OctA for immunoprecipitation and rabbit anti mTRP1-CT antibody for Western Blotting. C–E: Laser confocal microscopy on HEK293 cells stably expressing pIRES-EGFP alone as control or mTRP1β constructs. Localization of mTRP1β proteins was detected with monoclonal anti-FLAG antibody M2 and Cy5-labeled goat anti mouse. Shown are overlays of Cy5 (blue) and EGFP (green) (C), Cy5 (blue) and Bodipy TR-X thapsigargin (red) as a marker for the endoplasmatic reticulum (D) or Cy5 (blue) and the lipophilic dye CM-DiI (red) that stains the plasma membrane (E).
←

of either mutant failed to elicit a Ca^{2+} influx that would induce Ca^{2+} values significantly different from controls (Fig. 2C–F).

3.4. Cation currents in mTRP1β and mTRP1Δpp expressing HEK293 cells

To characterize the ion currents that may underlie the increases in $[Ca^{2+}]_i$ observed in fura-2 experiments, electrophysiological studies were performed with the patch-clamp technique in the whole-cell configuration. In light of the data presented in Fig. 2 (Ca^{2+} results), the electrophysiological studies were confined to control cells (expressing EGFP only), cells expressing wild-type mTRP1β and cells expressing the mTRP1Δpp mutant. HEK293 cells stably expressing mTRP1β exhibited inward currents that were significantly larger than in control cells (mTRP1β: -2.3 ± 0.50 pA/pF; control: -0.50 ± 0.36 pA/pF; $P < 0.05$; Fig. 3). The reversal potential was close to 0 mV (Fig. 4B) in the presence of asymmetrical Cl^- and Ca^{2+} concentrations, indicating that the currents were mainly carried by Na^+ in the inward direction and by Cs^+ in the outward direction. Inward currents were abolished when extracellular Na^+ was substituted with NMDG (Fig. 4). Thus, the currents were non-selective cation currents as already described for the human TRP1β (TRPC1A) in another expression system [3].

When the bath Ca^{2+} concentration was increased from 1.2 to 10 mM, inward currents declined considerably (Fig. 4A). This observation is likely to represent a block of mTRP1β, rather than inhibition, because outward currents were affected to a far smaller degree than inward currents (Fig. 4B). These effects of Ca^{2+} were completely reversible. Complete removal of Ca^{2+} from the bath by chelation with EGTA led to electrical instability already in control cells and was, therefore, not systematically studied in cells expressing mTRP1β.

Currents through mTRP1β were present right from the beginning of every experiment, i.e. immediately after obtaining the whole-cell configuration (Fig. 4A). Dialysis of the cytosol with EGTA (10 mM), or with EGTA and IP_3 (20 μM, $n = 11$), did not augment these currents that remained at a fairly stable plateau for several minutes. Addition of thapsigargin to the bath (1 μM) failed to induce a current increase within 3 min ($n = 5$). In contrast to wild-type mTRP1β, expression of mTRP1Δpp did not produce cation currents larger than in control cells (-0.19 ± 0.19 pA/pF; Fig. 3).

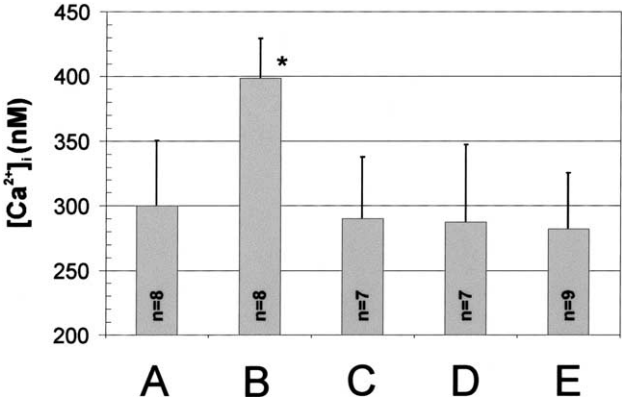

Fig. 2. Single cell Ca^{2+} flux measurements in CCh-stimulated HEK293 cells expressing mTRP1β and mutants. Changes in the cytosolic $[Ca^{2+}]_i$ concentration were measured in fura-2-loaded HEK293 cells stably expressing FLAG-tagged mTRP1β (B), mTRP1Δank (C), mTRP1Δcc (D) and mTRP1Δpp (E). As a control HEK293 cells transfected with pIRES2-EGFP only were used (A). Cells were assayed in Ca^{2+} free solution containing 0.5 mM EGTA and stimulated after 30 s with 200 μM CCh. Data (±S.E.) are maximal $[Ca^{2+}]_i$ following readdition of 1.8 mM Ca^{2+}. Each bar represents the mean Ca^{2+} entry following readdition of Ca^{2+} calculated from at least seven independent experiments with 14–20 responding cells per experiment (* denotes statistically significant difference versus vector control).

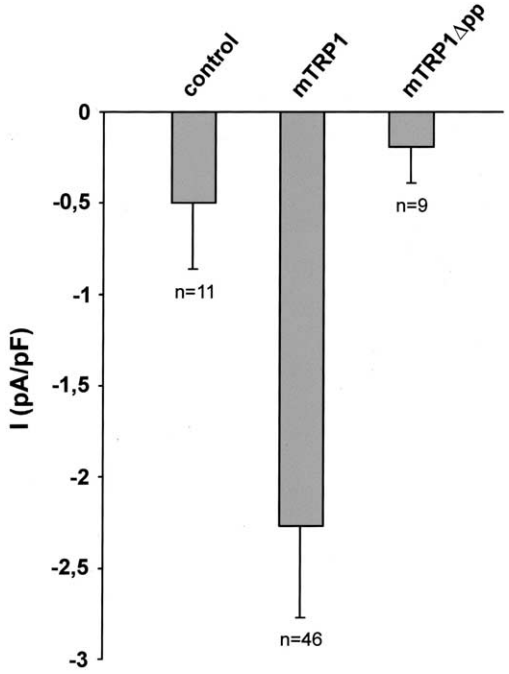

Fig. 3. Mean current densities in HEK293 cells stably expressing EGFP alone (control), as well as in cells expressing EGFP and additionally mTRP1β or mTRP1Δpp. The columns represent mean currents, expressed as NMDG-inhibitable part of inward currents at a holding potential of −60 mV and normalized to the cell capacitance. Numbers of individual experiments are given below the error bars (S.E.M.).

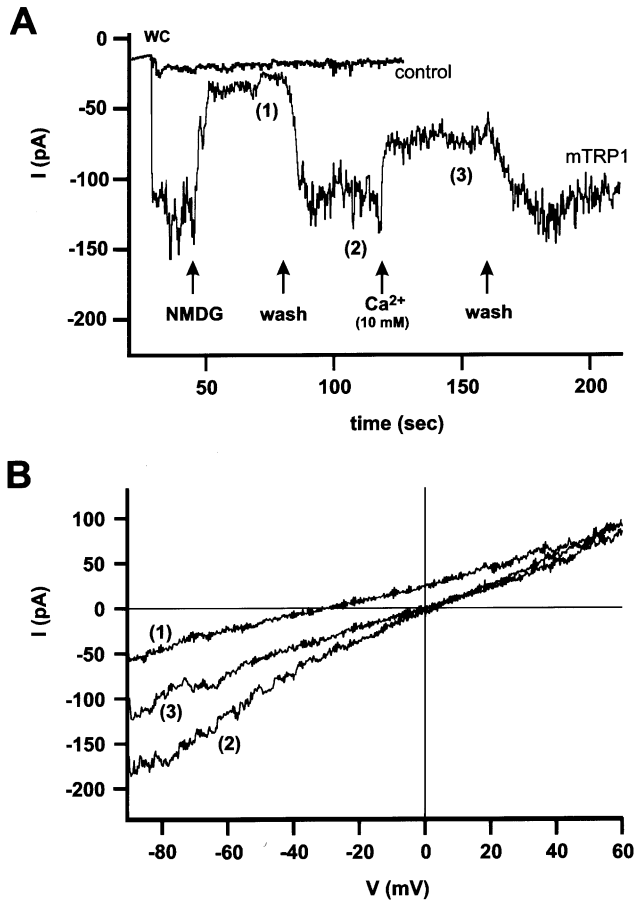

Fig. 4. Effects of expression of mTRP1β on Na^+ currents. A: Original current tracing from HEK293 cells stably expressing either EGFP alone (control) or EGFP together with mTRP1β. Currents were recorded after obtaining the whole-cell configuration (wc) at −60 mV. The cells were first exposed to a bath containing 140 mM Na^+ and than to a bath in which Na^+ was substituted by NMDG. The cells were furthermore exposed to a bath with 10 mM Ca^{2+}. Numbers in parentheses indicate the time at which the current–voltage relations shown in (B) were recorded. B: Current–voltage relation of currents in a mTRP1β expressing cell. The relations were obtained during the experiment shown in (A) by application of voltage ramps in the presence of three different bath solutions: (1) 150 mM NMDG and 1.2 mM Ca^{2+}; (2) 140 mM Na^+ and 1.2 mM Ca^{2+}; (3) 130 mM Na^+ and 10 mM Ca^{2+} as cations.

4. Discussion

The major finding of our present study is that the two domains within the N-terminal cytoplasmic tail, the coiled-coil domain and the ANK-repeats, have a significant importance for the formation of functional Ca^{2+} channels in HEK293 cells. Laser confocal microscopy studies clearly show that all mTRP1β constructs are correctly localized and orientated in the plasma membrane.

Fura-2 measurements of $[Ca^{2+}]_i$ in HEK293 cells stably transfected with mTRP1β revealed enhanced Ca^{2+} influx in a protocol that enables discrimination of Ca^{2+} entry across the plasma membrane from IP_3-induced Ca^{2+} release similar to results previously obtained by Zhu et al. [7] and Zitt et al. [3]. Based on our patch-clamp experiments mTRP1β forms non-selective cation channels. The currents were mainly carried by monovalent cations. In contrast to those in CHO cells [3] they were not activated by depletion of intracellular calcium stores and therefore resemble currents observed after expression of TRP1 in Sf9 insect cells [15]. It is noteworthy that several other members of the TRP family yield constitutively active currents when expressed in HEK293 cells, e.g. TRP3 [30], TRP5 [31] and TRP7 [32]. Another peculiar property of TRP1β in the system used is its response to increases in the extracellular Ca^{2+} concentration from 1.2 to 10 mM. With this maneuver, we planned to deduce the permeability to Ca^{2+} relative to that of Na^+. However, Ca^{2+} dramatically reduced inward currents. This effect did not represent a Ca^{2+}-mediated regulation of channel activity because currents in the outward direction were little affected. Therefore, the permeability of mTRP1β to Ca^{2+} could not be quantified with the patch-clamp technique. However the channels are obviously permeant to Ca^{2+}, as revealed by the measurements of $[Ca^{2+}]_i$.

In order to identify domains within mTRP1β that bear functional significance, we first performed studies in cells expressing a mTRP1β mutant lacking the pp region. This mutant failed to enable enhanced Ca^{2+} influx rates and cation currents, although it did not affect the structure of mTR1Pβ regarding the cytosolic localization of the C-terminus. Therefore, this region is indeed essential for functional channels but from our present experiments we cannot decide whether the pp region in fact participates in the forming of the channel pore.

Analysis of the primary structure of mTRP1β suggests two further candidate regions that may be relevant for the channel structure, the coiled-coil region and the region containing the three ANK-repeats. Hence, we constructed two further mutants lacking either of these regions. Although correctly inserted in the membrane both mutants do not form functional channels.

The structural significance of the coiled-coil region was further emphasized using the yeast two-hybrid system which demonstrated that this region facilitates homodimerization of the N-termini of mTRP1β. Dimerization was not found with the C-termini. Thus, we propose that the mTRP1β coiled-coil domain facilitates either homomerization of TRP1 or heteromerization with other coiled-coil domain containing proteins. Since N-terminal coiled-coil regions are conserved within the seven TRP proteins TRP1 to TRP7 (not shown), the same interaction may take place within several members of the TRP family.

ANK-repeats within the N-terminus were not required for dimerization in the yeast two-hybrid system, although expression of the respective mutant in HEK293 does not lead to enhanced Ca^{2+} influx. ANK-repeats are found in numerous proteins, including transcription regulators, cytoskeleton organizers and plant potassium channels [33] and have been found to mediate protein–protein interactions [19,20]. Interaction of ANK-repeats so far described only involve unrelated protein sequences, e.g. the PDZ (90 amino acid repeat first found in PSD-95 DIg ZO-1) domain [34]. From our present results it is tempting to speculate that potential interaction partners of the mTRP1 ANK-repeats either contribute to the regulation of the channel or its assembly and structure. Despite evidence for the interaction of the C-terminal domain of TRP proteins with the IP_3 receptor [35,36] no partner proteins have so far been identified for the N-terminal region of mTRP1β. Hypothetically, interaction with other proteins may

be cell-specific and may thus account for the discrepancies of TRP1 function observed in various cell types.

Acknowledgements: This work was funded by the Deutsche Forschungsgemeinschaft SFB 549 (project B6 to P.B. and J.F.) and SFB542 (project B5 to A.L. and C.Z.). Michael Engelke was partly funded by the Studienstiftung des Deutschen Volkes. Melanie Duckert is gratefully acknowledged for technical support. We kindly thank Stefanie Boese and Ilinca Ionescu for technical assistance. We are grateful to Alice McHardy for contributing some of the data obtained with the two-hybrid system.

References

[1] Wes, P.D., Chevesich, J., Jeromin, A., Rosenberg, C., Stetten, G. and Montell, C. (1995) Proc. Natl. Acad. Sci. USA 92, 9652–9656.
[2] Zhu, X., Chu, P.B., Peyton, M. and Birnbaumer, L. (1995) FEBS Lett. 373, 193–198.
[3] Zitt, C., Zobel, A., Obukhov, A.G., Harteneck, C., Kalkbrenner, F., Lückhoff, A. and Schultz, G. (1996) Neuron 16, 1189–1196.
[4] Sakura, H. and Ashcroft, F.M. (1996) Diabetologia 40, 528–532.
[5] Scott, K. and Zuker, C. (1998) Curr. Opin. Neurobiol. 8, 383–388.
[6] Hofmann, T., Schaefer, M., Schultz, G. and Gudermann, T. (2000) J. Mol. Med. 78, 14–25.
[7] Zhu, X., Jiang, M., Peyton, M., Boulay, G., Hurst, R., Stefani, E. and Birnbaumer, L. (1996) Cell 85, 661–671.
[8] Liu, X., Wang, W., Singh, B.B., Lockwich, T., Jadlowiec, J., O'Connel, B., Wellner, R., Zhu, M.X. and Ambudkar, I.S. (2000) J. Biol. Chem. 275, 9890–9901.
[9] Philipp, S., Trost, C., Warnat, J., Rautmann, J., Himmerkus, N., Schroth, G., Kretz, O., Nastainczyk, W., Cavalie, A., Hoth, M. and Flockerzi, V. (2000) J. Biol. Chem. 275, 23965–23972.
[10] Zitt, C., Obukhov, A.G., Strübing, C., Zobel, A., Kalkbrenner, F., Lückhoff, A. and Schultz, G. (1997) J. Cell Biol. 138, 1333–1341.
[11] Okada, T., Shumizu, S., Wakamori, M., Maeda, A., Kurosaki, T., Takada, N., Imoto, K. and Mori, Y. (1998) J. Biol. Chem. 273, 10279–10287.
[12] Hofman, T., Obukhov, A.G., Schaefer, M., Harteneck, C., Gudermann, T. and Schultz, G. (1999) Nature 397, 259–263.
[13] Vannier, B., Peyton, M., Boulay, M., Brown, G., Qin, N., Jiang, M., Zhu, X. and Birnbaumer, L. (1999) Proc. Natl. Acad. Sci. USA 96, 2060–2064.
[14] Garcia, R.L. and Schilling, W.P. (1997) Biochem. Biophys. Res. Commun. 239, 279–283.
[15] Sinkins, W.G., Estacion, M. and Schilling, W.P. (1998) Biochem. J. 331, 331–339.
[16] Vannier, B., Zhu, X., Brown, D. and Birnbaumer, L. (1998) J. Biol. Chem. 273, 8675–8679.
[17] Catterall, W.A. (1995) Annu. Rev. Biochem. 64, 493–531.
[18] Lupas, A. (1996) Trends Biochem. Sci. 21, 375–382.
[19] Michaely, P. and Bennett, V. (1993) J. Biol. Chem. 268, 22703–22709.
[20] Sedgwick, S.G. and Smerdon, S.J. (1999) Trends Biochem. Sci. 24, 311–316.
[21] Tuvia, S., Buhusi, M., Davis, L., Reedy, M. and Bennett, V. (1999) J. Cell Biol. 147, 995–1007.
[22] Xu, X.-Z.S., Li, H.-S., Guggino, W.B. and Montell, C. (1997) Cell 89, 1155–1164.
[23] Groschner, K., Hingel, S., Lintschinger, B., Balzer, M., Romanin, C., Zhu, X. and Schreibmayer, W. (1998) FEBS Lett. 437, 101–106.
[24] Mendelsohn, A.R. and Brent, R. (1994) Curr. Opin. Biotechnol. 5, 482–486.
[25] Laemmli, U.K. (1970) Nature 227, 680–685.
[26] Grynkiewicz, G., Poenie, M. and Tsien, R.Y. (1985) J. Biol. Chem. 260, 3440–3450.
[27] Hamill, O.P., Marty, A., Neher, E., Sakmann, B. and Sigworth, F.J. (1981) Pflügers Arch. 391, 85–100.
[28] Bobanovic, L.K., Laine, M., Petersen, C.C.H., Bennett, D.L., Berridge, M.J., Lipp, P., Ripley, S.J. and Bootman, M.D. (1999) Biochem. J. 340, 593–599.
[29] Andrade, W., Seabrook, T.J., Johnston, M.G. and Hay, J.B. (1996) J. Immunol. Methods 194, 181–189.
[30] Hurst, R.S., Zhu, X., Boulay, G., Birnbaumer, L. and Stefani, E. (1998) FEBS Lett. 422, 333–338.
[31] Yamada, H., Wakamori, M., Hara, Y., Takahashi, Y., Konishi, K., Imoto, K. and Mori, Y. (2000) Neurosci. Lett. 285, 111–114.
[32] Okada, T., Inoue, R., Yamazaki, K., Maeda, A., Kurosaki, T., Yamakuni, T., Tanaka, I., Shimizu, S., Ikenaka, K., Imoto, K. and Mori, Y. (1999) J. Biol. Chem. 274, 27359–27370.
[33] Daram, P., Urbach, S., Gaymard, F., Sentenac, H. and Chérel, I. (1997) EMBO J. 16, 3455–3463.
[34] Maekawa, K., Imagawa, N., Naito, A., Harada, S., Yoshie, O. and Takagi, S. (1999) Biochem. J. 337, 179–184.
[35] Tsiokas, L., Arnould, T., Zhu, C., Kim, E., Walz, G. and Sukhatme, V.P. (1999) Proc. Natl. Acad. Sci. USA 96, 3934–3939.
[36] Ma, H.-T., Patterson, R.L., van Rossum, D.B., Birnbaumer, L., Mikoshiba, K. and Gill, D.L. (2000) Science 287, 1647–1651.